JACS
JOURNAL OF THE AMERICAN CHEMICAL SOCIETY

Article

pubs.acs.org/JACS

Poly(*N*-isopropylacrylamide-*co*-tris-nitrilotriacetic acid acrylamide) for a Combined Study of Molecular Recognition and Spatial Constraints in Protein Binding and Interactions

Juan Liu, Mariana Spulber, Dalin Wu, Renee M. Talom, Cornelia G. Palivan,* and Wolfgang Meier*

Department of Chemistry, University of Basel, Klingelbergstrasse 80, Basel 4056, Switzerland

Supporting Information

ABSTRACT: Many biological processes require precise regulation and synergy of proteins, and consequently involve molecular recognition and spatial constraints between biomolecules. Here, a library of poly(*N*-isopropylacrylamide-*co*-tris-nitrilotriacetic acid acrylamide) (PNTs) has been synthesized and complexed with Cu^{2+} in order to serve as models for investigation of the combined effects of molecular recognition and spatial constraints in biomolecular interactions. The average distance between Cu^{2+}−trisNTA binding sites in PNTs polymers was varied from 4.3 to 31.5 nm by adjusting their trisNTA contents. His tag (His_6), His-tagged enhanced yellow fluorescent protein (His_6-eYFP), and His_6-tagged collagenase G (His_6-ColG), with sizes ranging from 1 to 11 nm, were used as models to assess whether the binding ability is influenced by a cooperative topology based on molecular recognition interactions with Cu^{2+}−trisNTA binding sites, and spatial constraints created by decreasing average distance between trisNTAs. His-tagged molecules bound to all PNTs polymers due to their molecular recognition interaction involving histidines and Cu^{2+}−trisNTA pockets, but with a binding ability that was highly modulated by the average distance between the trisNTA binding sites. Small molecular mass molecules (His_6) exhibit a high binding ability to all PNTs polymers, whereas his-tagged proteins bind to PNTs efficiently only when the average distance between trisNTA binding sites is larger than the protein dimensions.

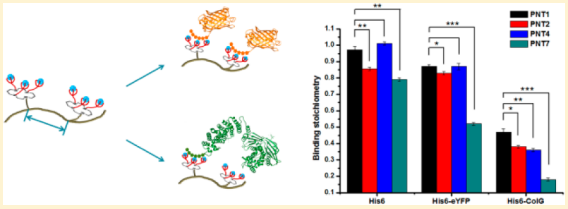

INTRODUCTION

The structures and functions of cells are critically dependent on association and dissociation interactions/processes, such as DNA replication and transcription,[1−3] cellular signaling,[4,5] and enzyme catalysis,[6] which simultaneously involve multiple molecules. The precise regulation of biological functions and processes is based on accurate molecular recognition interactions and spatial constraints between molecules.[7−9] Molecular recognition, determined by the exact geometric match between interacting molecules and the formation of complementary noncovalent bonds,[10] plays an important role in specific interactions between molecules.[11,12] In addition, the simultaneous interaction of multiple molecules is strongly dependent on spatial constraints when diverse binding sites of various ligands are located in the vicinity of each other.[7] In nature, a large number of proteins work together in pairs, and the interprotein distance influences their synergy.[13−15] For example, synergy is reduced when the distance between TATA-binding protein and initiator elements is large, whereas shorter distances induce stronger synergy and consequently higher activity.[16]

Although interactions and synergy of proteins can be successfully predicted by computer simulations,[17−19] the influence of distance constraints on binding and activity of biomolecules has been reported in only very few cases.[16] In addition, current computer simulations do not account for variations of physical properties, such as entropy, that are known to be crucial for molecular recognition.[20−23] Nano-structures based on self-assembled DNA have been used to study interligand distances resulting from the simultaneous binding of multiple ligands.[24,25] However, self-assembled DNA structures behave as rigid scaffolds, which induce a decrease in binding due to spatial mismatches.[24,25] To the best of our knowledge, there are very few model scaffolds that can specifically bind multiple proteins with controlled distances between binding sites, and none has used polymer-based scaffolds.

Various polymers have been used for protein conjugation by covalent bond formation,[26−28] or noncovalent interactions attributed to molecular recognition.[29−33] In particular, tris-nitrilotriacetic acid (trisNTA) functionalized polymers have been used to bind His-tagged proteins with multiple metal−NTA coordination pockets due to the high affinity.[34−44] As His tag normally is expressed on either the N- or C-terminus of proteins, far away from their active centers, the binding does not influence their activities.[38,45−47] For example, trisNTA functionalized poly(butadiene)-*block*-poly(ethylene oxide) binds to His-tagged enhanced green fluorescent protein (His_6-eGFP) without affecting its fluorescence,[38,47] and His-tagged laccase preserved its activity when interacting with Ni^{2+}−NTA immobilized on its surface.[46] However, to the best of our knowledge, the functionalization of polymers by trisNTA is limited to the terminal ends of the polymers.[37,47] Therefore,

Received: April 11, 2014
Published: August 21, 2014

   dx.doi.org/10.1021/ja503632w | *J. Am. Chem. Soc.* 2014, 136, 12607−12614

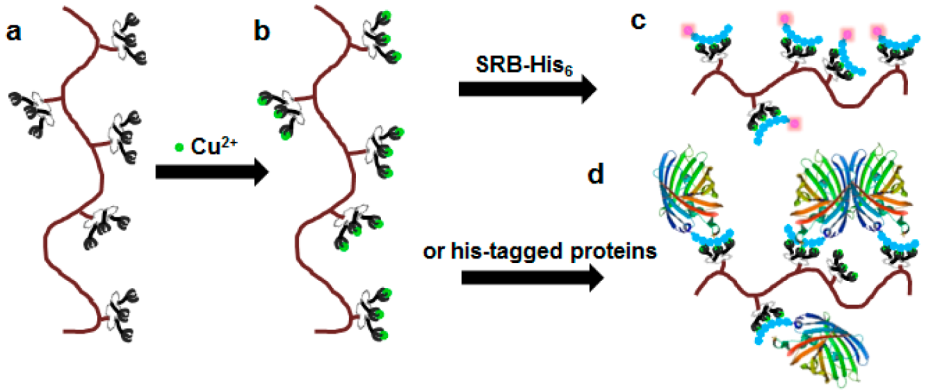

Figure 1. Schematic representation of PNTs, which coordinate Cu^{2+}, and further bind to sulforhodamine B labeled His_6 (SRB-His_6), His_6-eYFP, and His_6-ColG.

Scheme 1. Synthesis of Prot−trisNTA and PNT Copolymers

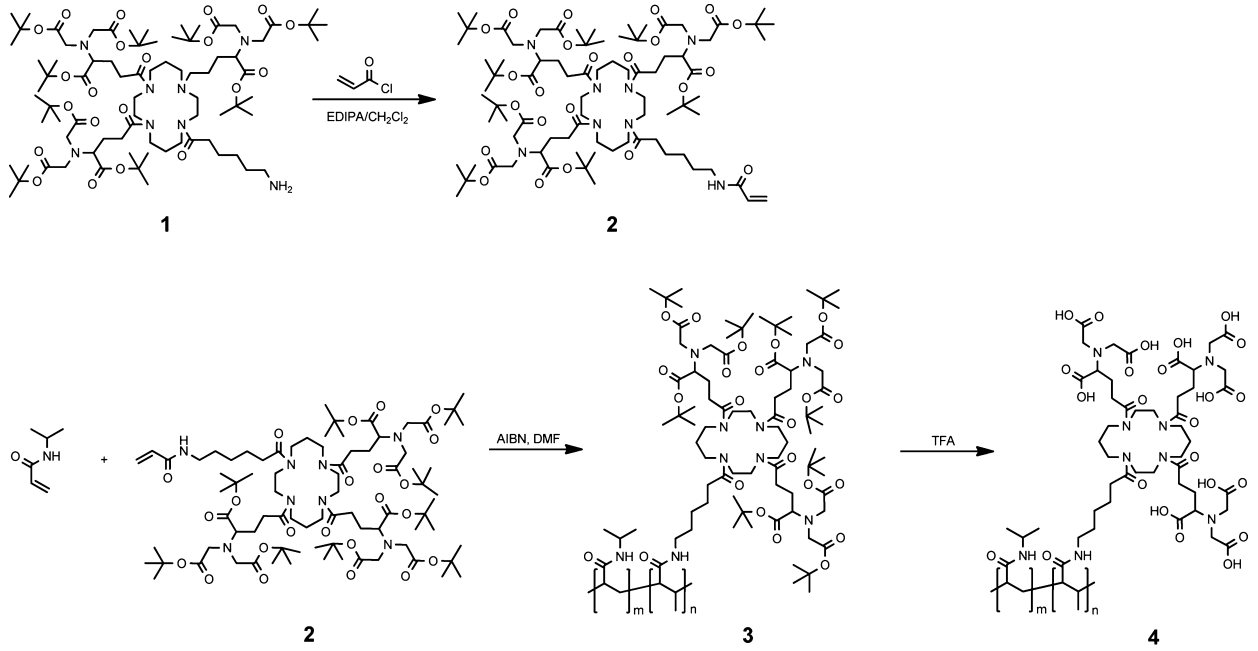

polymer−His-tagged protein interactions have been studied only in relation to their binding affinity via molecular recognition interactions at a single, specific metal−NTA pocket. An influence of distance between the NTA pockets on His-tagged proteins binding was only considered when NTA pockets were exposed at the surface of polymer vesicles.[38]

Here, we have synthesized a library of novel poly(*N*-isopropylacrylamide-*co*-tris-nitrilotriacetic acid acrylamide) polymers (PNTs), and complexed them with Cu^{2+} to serve as flexible models to assess the combined effect of molecular recognition and spatial constraints in binding specific molecules ranging from small molecular mass molecules (<1 kDa) up to proteins (Figure 1). This library of PNTs provides different average distances between trisNTA sites, which can modulate the binding of multiple molecules as a function of their size. We selected His_6, His-tagged enhanced yellow fluorescent protein (His_6-eYFP) and His-tagged collagenase G (His_6-ColG) as model molecules because they provide a large range of sizes (from 1 to 11 nm). First, the coordination of copper to trisNTA pockets was characterized by Fourier transform infrared spectroscopy (FTIR), UV−vis spectroscopy, and electron paramagnetic resonance (EPR). Then, the binding of His-tagged molecules to trisNTA was analyzed by fast protein liquid chromatography (FPLC), FTIR, isothermal titration calorimetry (ITC) and EPR. We investigated the binding affinity, and intermolecular interactions of His-tagged molecules bound to the polymers as a function of the specific local topology. Our polymers provide a dual topologic match at the molecular level involving both molecular recognition at trisNTA pockets, and steric effects regulated by the distance between the trisNTA sites. In this way it is possible to get an insight into the fine details of binding affinities of molecules, which are regulated not only by attachment to a specific target, but also by spatial constraints.

The concept of polymers serving as models for combined geometric topology with size requirements is expected to show the real binding capacity of molecules to a complex targeting configuration, which mimics biological systems in important details.

PNT copolymers with high trisNTA mol % have a short average distance between trisNTA binding sites, and are expected to influence the binding ability and binding affinity

dx.doi.org/10.1021/ja503632w | J. Am. Chem. Soc. 2014, 136, 12607−12614

Table 1. Polymerization of PNTs, Molecular Mass, and Polydispersity

	Polymerization of protected PNTs							
	prot−trisNTA (mol %)				GPC results		deprotection	
polymer code	in feed	in polymer[a]	in polymer[b]	yield (%)	M_n (× 10^4)	M_w/M_n	yield (%)	M_n[c] (× 10^4)
PNT7	10.0	8.3	6.8	60	3.00	1.8	95	2.47
PNT4	5.0	4.2	4.1	63	2.95	1.8	69	2.59
PNT2	3.0	2.3	1.9	56	2.68	1.7	96	2.47
PNT1	1.0	0.8	0.8	55	3.45	1.7	94	3.34
PN	0	0	-	62	2.48	1.7	-	-

[a]Calculated based on integration of the ^{1}H NMR spectrum. [b]Evaluated by acid−base titration. [c]The values were calculated based on the molecular mass, and polymer degree of protected PNTs obtained by GPC and ^{1}H NMR results, respectively.

between His-tagged molecules and trisNTA pockets, whereas PNT copolymers with low trisNTA mol % are expected to not influence the binding of His-tagged molecules.

RESULTS AND DISCUSSION

Synthesis and Characterization of PNT Copolymers. *t*-Butyl ester protected PNTs (**3**) with different distances between trisNTA moieties were synthesized by free radical polymerization of *N*-isopropylacrylamide (Nipam) and *t*-butyl ester protected tris-nitrilotriacetic acid acrylate (prot-trisNTA) (**2**) using azobisisobutyronitrile (AIBN) as initiator (Scheme 1). PolyNipam (PN) was chosen due to its high hydrophilicity and biocompatibility.[48] Molar ratios of prot-trisNTA and Nipam in the range 1:99 and 10:90 were used for the polymerization in order to obtain polymers with different distances between trisNTA binding sites (Table 1). The formation of PNT copolymers with different trisNTA mol % was established by ^{1}H NMR (Supporting Information Figure S2). The characteristic peaks of prot-trisNTA present at δ = 3.44 ppm, δ = 3.50 ppm, δ = 1.48 ppm and δ = 1.45 ppm correspond to protons on the trisNTA scaffold and the *t*-butyl ester group,[49] while the Nipam peaks at δ = 4.00 ppm and δ = 1.16 ppm correspond to protons on −CH− and methyl groups.[50] TrisNTA contents of 0.8−8.3 in all copolymers were calculated from the ratios between the integrals of the peaks at δ = 3.44 ppm and δ = 3.50 ppm (from trisNTA), and the peak at δ = 4.00 ppm (from −CH− of Nipam) (Supporting Information Figure S2).

^{1}H NMR peaks at δ = 1.43 ppm and δ = 1.40 ppm (characteristic of *t*-butyl ester groups) disappeared after the deprotection of the polymers, indicating a total deprotection (Supporting Information Figure S3). We used an acid−base titration to estimate the total trisNTA content (Table 1). These values were slightly lower than those obtained from ^{1}H NMR, because ^{1}H NMR can induce some systematic errors in the estimation of the molar ratio of trisNTA/Nipam repeating units in polymers, due to baseline distortion.[51] Thus, we used the trisNTA mol % values obtained from acid−base titration for subsequent calculations.

Effect of Temperature and pH on the Aggregation Behavior of PNTs. It is important to understand the factors which might affect the binding affinity, such as the stimuli-responsiveness of copolymer. As PN is thermoresponsive (with a low phase transition temperature around 32 °C),[50,52] and becomes pH-dependent after copolymerization with acrylic acid derivatives,[52] the phase transition of the library of PNT copolymers was assessed by UV−vis spectroscopy (Figure 2). In contrast to PN and copolymers composed of Nipam and acrylic acid derivatives, such as poly(Nipam-*co*-acrylic acid),[53]

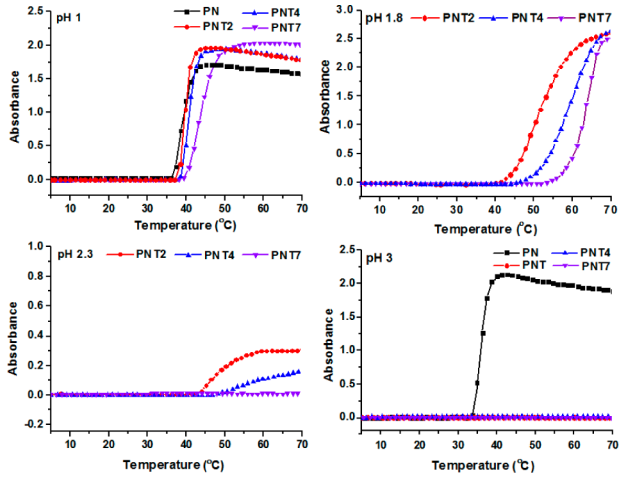

Figure 2. Absorbance dependence of temperature (5−70 °C) for PNT copolymers (1 mg/mL) at pH 1−3. His_6 binding behavior of trisNTA units from PNT copolymer.

all PNT polymers showed no phase transition at pH > 3, because of the low pK_a values of NTA (1.9, 2.5, and 9.7).[54] TrisNTA units (67%) are ionized at pH > 3, resulting in a significant increase in hydrophilicity of the PNTs. At pH values <2.3, below the pK_{a2} of NTA, trisNTA is partly protonated and exhibits hydrophobicity, resulting in a phase transition for PNT2 and PNT4. PNT7 with 6.8 mol % trisNTA showed thermoresponsive behavior at pH values <1.8. A sharp phase transition for all five PNT copolymers was observed at pH 1.0. As the experiments were conducted in PBS buffer at room temperature, there was likely no aggregation of the PNTs copolymers.

Binding of His_6 to PNT Copolymers. Cu^{2+} was first coordinated to PNTs in order to serve as a binding center for His_6. A stoichiometry of 3:1 for Cu^{2+}:trisNTA indicates that the copolymerization did not affect the accessibility of the trisNTA pockets as proved by UV−vis and FTIR (Supporting Information Figure S4−S6).

In a second step, the binding of His_6 to Cu^{2+}-loaded PNTs was assessed by FPLC (Supporting Information Figure S7) and FTIR (Supporting Information Figure S8). We labeled His_6 with sulforhodamine B (λ_{max}= 570 nm) for FPLC analysis. PNT copolymers showed no absorbance at 570 nm, and eluted faster than SRB-His_6 due to their higher mass. On the basis of the integral area, the number of trisNTA:His_6 ("binding stoichiometry") was determined to be 1:1 for all PNT1 to PNT4 copolymers, in agreement with the reported values for trisNTA and His_6.[49] Only in the case of PNT7−SRB−His_6 was a binding stoichiometry of 1:0.8 obtained (Supporting

dx.doi.org/10.1021/ja503632w | J. Am. Chem. Soc. 2014, 136, 12607−12614

Information Figure S7). The decrease in average distance between trisNTA binding sites sterically hinders the binding of His_6 to the NTA pocket, and results in a slightly decreased binding stoichiometry. The binding stoichiometry values are in agreement with those obtained by ITC (Supporting Information Figure S14).

EPR spectroscopy was used to investigate the Cu^{2+} coordination sphere when complexed to trisNTA on PNT polymers, and after addition of His_6, since the spectral parameters are known to change upon modification of the metal coordination sphere inside the NTA pocket induced by complexation with His_6.[47] Different model systems were studied and compared: $CuCl_2$ in solution (a), and mixtures of Cu^{2+} with PN, His_6, with trisNTA (c), with PNT1 (g) and with both PNT1 and His_6 (i) (Figure 3, and Table 2) along with the corresponding computer simulations (Figure 3b, d, e, f and i). The Cu^{2+} EPR spectrum in the presence of PN was similar to that for free Cu^{2+}, which indicates that the metal is not coordinated by the polymer chain. In the presence of His_6 and trisNTA two species were detected: one similar to free Cu^{2+}, and one with g_z and A_z values similar to those reported for the Cu^{2+} complexes of these molecules.[38] In the case of Cu^{2+} complexation with PNT1 polymer, only one species was detected (Figure 3g) with spectral parameters indicative of tetragonal symmetry[55] and similar to those for the Cu^{2+} complexation of trisNTA;[38] thus, the Cu^{2+} coordination sphere involves three carboxyl groups and one amine group. The value of g and A tensors indicate a tetragonal symmetry.[55] When His_6 was added to Cu^{2+}:PNT1, the EPR spectrum changed significantly (Figure 3i). The signal was poorly resolved due to a significant broadening. The values of both g and hyperfine coupling differ from those observed for the Cu^{2+}:PNT1 mixture, and are similar to the hyperfine coupling constants reported for Cu^{2+} dimers (A_x 27 G, A_y 38 G and A_z 82 G).[56] The formation of the dimers is also sustained by the signal recorded at half-field, which is typical for dimeric Cu^{2+} (Supporting Information Figure S9). A similar behavior was described for Cu^{2+}:NTA:His_6 mixtures, where the formation of Cu^{2+} dimers was proposed.[38]

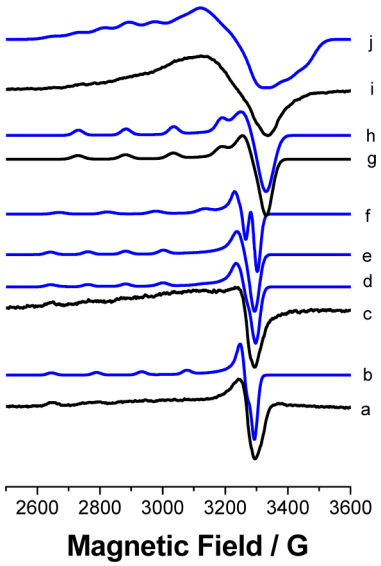

Figure 3. (a) X-band CW-EPR spectra of frozen solution in distilled water at 100 K together with their simulations using the EPR parameters indicated in Table 2: CuCl2 solution (a), and the related simulation of its EPR spectrum (b), Cu^{2+}–trisNTA mixture (c) with the related simulation of the EPR spectrum (d), Cu^{2+}–PNT1 mixture (g) with the related simulation of EPR spectrum (h), Cu^{2+}–PNT1:His_6 mixture (i) with the simulation of its EPR spectrum (j). (e and f) Individual contributions of paramagnetic species to the simulation (d). All EPR spectra are normalized for presentation means.

To investigate whether His_6 can induce formation of cross-linked PNT copolymers, we used dynamic light scattering (DLS) before and after His_6 complexation. The values of the hydrodynamic radius (R_h) of PNT copolymers were measured as being in the range 3–4 nm, in agreement with R_h value of PN with a similar degree of polymerization,[57] and they did not change after His_6 complexation (Supporting Information Figure S10). There were no obvious changes in the hydrodynamic radius after His_6 coordination to Cu^{2+}–trisNTA, suggesting that only one His_6 can bind to one trisNTA–Cu^{2+} pocket, and that there was no aggregation of His_6–Cu^{2+}–trisNTA copolymers in the solution.

Binding Ability of His-Tagged Proteins to the PNTs. To understand the influence of spatial constraints on the binding ability of molecules with high MW, we investigated the binding of two His-tagged proteins, His_6-eYFP and His_6-ColG to the PNT copolymers with different distance between the trisNTA binding sites. Binding of proteins to Cu^{2+}–trisNTA sites was assessed in physiological conditions in order to preserve the natural conformation of proteins.[73,74] The dimensions of monomeric eYFP and monomeric ColG are 3 nm × 4 nm and 7 nm × 11.5 nm, respectively,[58,59] The

Table 2. EPR Spectral Parameters for Frozen Solutions of Cu^{2+} in $CuCl_2$, Cu^{2+}–TrisNTA, Cu^{2+}–His_6, Cu^{2+}–PN, Cu^{2+}–PNT1, and Cu^{2+}–PNT1–His_6 Complexes[a]

	g_x, g_y	g_z	$\lvert A_x\rvert$, $\lvert A_y\rvert$/G	$\lvert A_z\rvert$/G
$CuCl_2$	2.080	2.38	5	140
$Cu(Cl)_2$:PN	2.083	2.38	5	142
$Cu(Cl)_2$:His_6 (3:1)	2.082, 2.089	2.42	5	115
	2.082	2.28	5	120
$Cu(OTf)_2$:His_6 (1:5)[34]	2.074	2.37	5	105
$Cu(Cl)_2$:trisNTA (3:1)	2.082, 2.090	2.41	10, 15	120
	2.089, 2.100	2.34	10, 5	154
$Cu(OTf)_2$:trisNTA (1:5)[34]	2.061	2.302	10	120
$Cu(Cl)_2$:PNT1	2.068	2.30	10	154
$Cu(Cl)_2$:PNT1:His_6	2.062, 2.080	2.35	30, 35	80

[a]The hyperfine values are given for the ^{63}Cu nucleus.

dx.doi.org/10.1021/ja503632w | J. Am. Chem. Soc. 2014, 136, 12607–12614

reactivity ratios of trisNTA ($r_{trisNTA}$) and Nipam (r_{Nipam}) were determined by the Fineman−Ross method using ^{1}H NMR data (Supporting Information Figure S11−12). The r_{Nipam} value of 1.35 is only slightly larger than the $r_{trisNTA}$ value of 0.8. To keep a constant trisNTA mol % in copolymers, and to avoid production of block-like copolymers, the conversion of all PNT copolymers was controlled to be below 65% (Supporting Information Figure S13). As expected, trisNTA groups are statistically distributed on the polymer chains. We considered a homogeneous distribution of trisNTA groups on the polymer chain, and neglected possible statistical agglomeration due to the random character of polymerization.[61−63] The average distances between the trisNTA−Cu^{2+} binding sites of PNTs were calculated by molecular dynamic calculations based on a minimum energy conformation. This 3D model describes in a first approximation the average distance between the trisNTA sites because repulsive forces associated with the trisNTA sites are expected to favor a Langevin dependence of elongation on force, and favor a stretch chain conformation. Compared to a normal random coil model of the polymer chain, the charges on PNTs associated with trisNTA sites determine that different chain conformations are no longer equally probable because they correspond to energies of the chains in the fields produced by the electrical charges (Langevin dependence). Indeed, zeta potential measurements proved the charged character of polymers in PBS buffer, due to the presence of metal−trisNTA sites (Supporting Information Table S3). Theoretical average distance values varied from 31.5 to 4.3 nm for PNT1−7 (Supporting Information Table S1). Note that these values are larger than the real distance between two neighboring trisNTA sites in solution due to the 3D conformation of PNTs. The average distance approaches the real distance value only when the trisNTA sites are close to each other, as in the case of PNT4 and PNT7.

To investigate the influence of spatial constraints on the binding ability of His-tagged proteins to PNTs, we used ITC (Figure 4, Supporting Information Figure S14). The highest binding stoichiometry for both His_6-eYFP and His_6-ColG (0.87 and 0.47) was determined for PNT1, which has the largest distance between trisNTA sites. Decreasing the distance between triNTA−Cu^{2+} groups had no influence on the binding stoichiometry of His_6-eYFP, due to its relatively small size, but evidently reduced the binding stoichiometry of His_6-ColG from 0.47 to 0.36. For PNT7, which has the smallest distance between trisNTA sites, a dramatic decrease in binding stoichiometry was observed for both His_6-eYFP and His_6-ColG (0.51 and 0.18, respectively). This significant decrease was expected because of the inaccessibility of trisNTA−Cu^{2+} binding sites due to their close packing, which prevents coordination of high MW molecules. The low binding stoichiometry of His_6-ColG to PNTs could be the consequence of His_6-ColG dimer formation, which inhibits the binding to PNTs (Supporting Information Figure S16). An interesting observation is that proteins and polymers are able to arrange themselves to obtain maximal binding. When the average distance between trisNTA binding sites is decreased to 5.2 nm (PNT4), which is closer to the size of eYFP, the binding stoichiometry of the protein does not change. We attribute the binding stoichiometry, in the case of PNT4, to the flexibility of the polymer chain and a 3-D structure rearrangement, which allow the binding of eYFP even though their size is close to the maximal average distance between the trisNTA sites. This is in agreement with previous reports, which indicated that polymers with multiple ligands are able to bind multiple proteins on each polymer chain.[45,60] When the average distance decreases to the size of eYFP, as in the case of PNT7, the number of proteins bound to the polymer chain is not increased, as would have been expected by the increased number of trisNTAs/polymer chain. We suppose that in this case the 3D conformation of PNT7 in solution induces spatial limitations, which do not favor a topologic match between trisNTA sites and eYFP. The binding stoichiometry of His_6-ColG to PNT2 is only slightly higher than that to PNT4, due to the low number of ColG proteins/polymer chain, which prevents the distance constraints from playing a role in protein binding (Supporting Information Table S2).

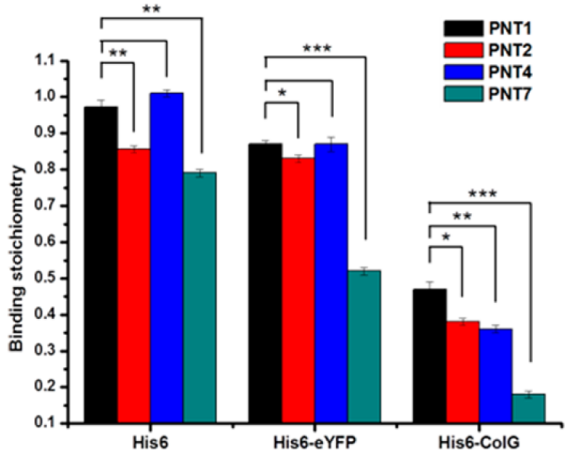

Figure 4. Binding stoichiometry between trisNTA−Cu^{2+} groups in PNTs and His_6, His_6-eYFP and His_6-ColG. Asterisks indicate significance in two-tailed Student's t test: *P < 0.05, **P < 0.005, ***P < 0.0005.

PNTs copolymers possess higher binding capacity to small MW molecules than to large molecules, as expected. Although PNT7 has the highest trisNTA mol %, the binding capacity to his-tagged proteins is lower than that for PNT4 because of the spatial constraint (Supporting Information Table S4).

Binding Affinity of His-Tagged Molecules to PNTs. High binding affinity is crucial in nature for the binding of multiple proteins. For example, Bcd protein is able to position at a distance close to 10 base pairs on DNA when the binding affinity is high, whereas the binding site arrangements of the Bcd protein decreases rapidly when the binding affinity is decreased.[61] Therefore, the binding affinity is an essential parameter for indicating the binding of multiple proteins, and for studying the effect of spatial constraints. We chose trisNTA for protein binding because of its high binding affinity for His tag and His-tagged proteins.[38,49,62] To investigate whether conjugation of trisNTA to polymers and the spatial constraint between the trisNTA sites affect the binding affinity of his-tagged molecules, we determined the dissociation constant (K_D) values. The K_D value obtained for His_6 bound to trisNTA on PNTs are similar to that obtained for trisNTA−Cu^{2+}−His_6 (Table 3), which suggests that the conjugation of polymer to trisNTA does not influence the binding affinity to His_6. A higher K_D (0.6 ± 0.2 μM) value was reported for His_6 bound to trisNTA-modified polymer vesicles, due to the presence of surrounding poly(ethylene oxide) brushes at the surface of the polymer vesicles.[38] Interestingly, the binding affinity of different His-tagged molecules to PNT1 was not affected by the

dx.doi.org/10.1021/ja503632w | J. Am. Chem. Soc. 2014, 136, 12607−12614

Table 3. K_D for the Binding between TrisNTA Functionalized Polymers and His-Tagged Molecules

	K_D (μM)[a]		
	His_6	His_6-eYFP	His_6-ColG
PNT1-Cu^{2+}	0.30 ± 0.02	0.15 ± 0.02	0.35 ± 0.06
PNT2-Cu^{2+}	0.17 ± 0.01	0.26 ± 0.03	0.26 ± 0.03
PNT4-Cu^{2+}	0.13 ± 0.01	0.33 ± 0.06	0.20 ± 0.04
PNT7-Cu^{2+}	0.10 ± 0.01	0.07 ± 0.01	0.20 ± 0.04
TrisNTA-Cu^{2+}	0.39 ± 0.03		

[a] K_D values presented in this paper were determined by ITC measurements.

structure or the size of His-tagged molecules, but spatial constraint played an active role in the binding affinity between trisNTA and His-tagged molecules. When the distance between the binding sites was reduced, a decrease in K_D was observed for all His-tagged molecules. This suggests hydrogen bond formation between His-tagged molecules which decreases their separation, and thus influences their binding.[45] It has been reported that the binding affinity of proteins can be enhanced when they are located closer to each other on a surface.[63,64] PNTs have a higher binding affinity to His-tagged proteins compared to other trisNTA-functionalized polymers,[47,62] because Cu^{2+} was used as coordination ion instead of Ni^{2+}, and it is known to favor stronger binding than Ni^{2+}.[38]

Influence of Spatial Constraints on Interactions of Bound His-Tagged Molecules. To get more information on the interactions between His-tagged molecules and PNTs, we assessed the change of enthalpy ($\Delta H°$) and entropy ($\Delta S°$) (Table 4).[65,66] For PNT1−Cu^{2+}−His_6 and PNT2−Cu^{2+}−His_6 complexes, the value of $\Delta H°$ is similar to that obtained for trisNTA−Cu^{2+}−His_6 (Table 4), suggesting that the coordination between trisNTA−Cu^{2+} and His_6 is the only interaction when His_6 binds PNTs copolymers. With decreasing distance between trisNTA binding sites, $\Delta H°$ increases, and $\Delta S°$ decreases, due to formation of hydrogen bonds between neighboring His_6 units, and a conformation restriction of the polymer chain.[67,68] Short distances and hydrogen bond formation between His_6 units inhibit access to several trisNTA binding sites, and lead to decreases in binding stoichiometry for the case of PNT7 (as shown both by ITC and FPLC).

The binding behavior between PNTs and His-tagged proteins is more complicated. When His_6-eYFP was bound to PNTs, low $\Delta H°$ (3.6 kcal/mol), and positive $\Delta S°$ values (19.3 cal/mol/K) were obtained. No influence of the secondary structure of His_6-eYFP was observed by Circular dichroism (CD) spectroscopy after the coordination of PNTs (Supporting Information Figure S15). A possible explanation for the positive $\Delta S°$ values is that His_6 was not freely exposed, but interacted with eYFPs.[69,70] The binding of His_6 to PNTs affected the interaction between His_6 and eYFP, and caused a total increase of $\Delta S°$. The decrease in distance between trisNTA sites induced a decrease in $\Delta S°$, due to restrictions in rotation and translation of the binding proteins.[71] When the distance between trisNTA sites was further decreased (PNT7), the number of proteins bound to PNTs copolymers was unchanged (Supporting Information Table S2), and therefore $\Delta S°$ remained constant (Table 4). This indicates that no additional proteins are able to bind to the polymer due to the limited space, even though the number of trisNTA sites is increased.

In contrast to PNT−Cu^{2+}-eYFP complexes, His_6-ColG binding to PNT1 is accompanied by an increase in $\Delta H°$ to a value of 31.7 kcal/mol, due to the formation of hydrogen bonds between PNTs and the protein molecules. The decrease in space between trisNTA sites induced an increase in $\Delta H°$ from 31.7 to 60.0 kcal/mol, which was compensated by a large decrease in $\Delta S°$ from −87.6 to −177 cal/(mol/K). The decrease in $\Delta S°$ is possibly the result of oligomerization of the proteins, as has been shown for the fibroblast growth factor 8b.[45] Oligomerization of proteins reduces the translational and rotational degrees of freedom, and induces a reduction in $\Delta S°$.[72]

CONCLUSIONS

We synthesized and characterized a library of new poly(*N*-isopropylacrylamide-*co*-tris-nitrilotriacetic acid acrylamide) polymers containing multi-trisNTA binding sites with different average distances between them. After complexation with copper, PNTs copolymers were used as models to assess the combined effect of molecular recognition and spatial constraints on the binding of molecules ranging from small molecular mass compounds up to proteins. Small molecular mass molecules (His_6) can easily access and bind to trisNTA sites of the polymers: a high binding ability of all PNT polymers was obtained, independent of the average distance between the trisNTA sites. A different situation was found in the case of protein binding. His_6-eYFP binds efficiently to PNTs only when the average distance between the trisNTA sites is larger than the protein size. The lowest binding stoichiometry was determined for interaction of His_6-ColG with PNTs, due to the protein size (11 nm) and its possible dimerization. By controlling the amount of trisNTA on PNT polymers, we have efficiently controlled the binding stoichiometry, their affinity for selected his-tagged molecules, and their interactions in real conditions mimicking those encountered in biology.

These novel polymers containing multi-trisNTA binding sites with different average spaces between them open a wide field of possible applications as scaffolds for multibinding of His-tagged proteins, or combination therapy. By selecting an appropriate

Table 4. Enthalpy ($\Delta H°$) and entropy ($\Delta S°$) of interactions between PNTs (or trisNTA) and His-tagged molecules

	$\Delta H°$ (kcal/mol)[a]			$\Delta S°$ (cal/(mol/K))[a]		
	His_6	His_6-eYFP	His_6-ColG	His_6	His_6-eYFP	His_6-ColG
TrisNTA-Cu^{2+}	−20.7 ± 0.3			−40.1		
PNT1-Cu^{2+}	−19.4 ± 0.2	−3.6 ± 0.1	−31.7 ± 1.8	−35.3	19.3	−87.7
PNT2-Cu^{2+}	−19.8 ± 0.2	−4.7 ± 0.1	−37.6 ± 1	−35.3	14.3	−89.5
PNT4-Cu^{2+}	−23.0 ± 0.1	−6.0 ± 0.1	−42.9 ± 1.7	−45.5	9.5	−123.0
PNT7-Cu^{2+}	−25.8 ± 0.2	−6.8 ± 0.1	−60.0 ± 5.0	−54.4	9.9	−177.0

[a] $\Delta H°$ and $\Delta S°$ were determined by ITC measurements.

dx.doi.org/10.1021/ja503632w | J. Am. Chem. Soc. 2014, 136, 12607−12614

PNT with a known average distance between the trisNTA sites and His-tagged proteins with a specific size, it is possible to predict the number of proteins bound per PNT chain, as well as their binding affinity. In addition, PNTs can be used to preorganize proteins to favor encapsulation of proteins inside polymeric vesicles and cellular uptake.

■ ASSOCIATED CONTENT

Supporting Information

Materials, characterization of trisNTA acrylate monomer and PNTs, protein expression and analysis, and additional characterization results. This material is available free of charge via the Internet at http://pubs.acs.org.

■ AUTHOR INFORMATION

Corresponding Authors

cornelia.palivan@unibas.ch
wolfgang.meier@unibas.ch.

Notes

The authors declare no competing financial interest.

■ ACKNOWLEDGMENTS

We thank Swiss National Science Foundation, and University of Basel for financial support. J.L. thanks China Scholarship Council for supporting the fee to study abroad. We thank Prof. Anatole von Lilienfeld and Dr. Raghunathan Ramakrishnan for the computational simulation of the 3D polymer conformation. We thank Biozentrum Biophysics Facility Basel for the use of their ITC instrument. We thank Prof. Nico Bruns from AMI Fribourg for providing the plasmids of eYFP and discussions. J.L. acknowledges Matthias Knop from University of Basel, Dr. Rolf Jaussi and Dr. Philipp Berger from Paul Scherrer Institute and Dr. Alejandro Fernandez-Estrada from Biozentrum Basel for information regarding His-tagged proteins. J.L. thanks Gesine Gunkel-Grabole, Patric Baumann, Fabian Itel, Martin Nussbaumer, Adrian Najer, Jason Duskey and Anja Car from University of Basel for useful discussions. Authors thank Dr. B.A. Goodman for editing the manuscript.

■ REFERENCES

(1) Chagin, V. O.; Stear, J. H.; Cardoso, M. C. *Cold Spring Harbor Perspect. Biol.* **2010**, *2*, 4.
(2) Costa, A.; Hood, I. V.; Berger, J. M. *Annu. Rev. Biochem.* **2013**, *82*, 25.
(3) Falkenberg, M.; Larsson, N. G.; Gustafsson, C. M. *Annu. Rev. Biochem.* **2007**, *76*, 679.
(4) Bailly-Bechet, M.; Borgs, C.; Braunstein, A.; Chayes, J.; Dagkessamanskaia, A.; François, J.-M.; Zecchina, R. *Proc. Natl. Acad. Sci. U.S.A.* **2011**, *108*, 882.
(5) Scott, J. D.; Pawson, T. *Science* **2009**, *326*, 1220.
(6) Benkovic, S. J.; Hammes-Schiffer, S. *Science* **2003**, *301*, 1196.
(7) Baron, R.; McCammon, J. A. *Annu. Rev. Phys. Chem.* **2013**, *64*, 151.
(8) Mammen, M.; Choi, S.-K.; Whitesides, G. M. *Angew. Chem., Int. Ed.* **1998**, *37*, 2754.
(9) Zhu, X.; Gerstein, M.; Snyder, M. *Genes Dev.* **2007**, *21*, 1010.
(10) Fersht, A. R. *Trends Biochem. Sci.* **1987**, *12*, 301.
(11) Eck, M. J.; Pluskey, S.; Trub, T.; Harrison, S. C.; Shoelson, S. E. *Nature* **1996**, *379*, 277.
(12) Katchalski-Katzir, E.; Shariv, I.; Eisenstein, M.; Friesem, A. A.; Aflalo, C.; Vakser, I. A. *Proc. Natl. Acad. Sci. U.S.A.* **1992**, *89*, 2195.
(13) Vardhanabhuti, S.; Wang, J.; Hannenhalli, S. *Nucleic Acids Res.* **2007**, *35*, 3203.
(14) Chiang, D.; Nix, D.; Shultzaberger, R.; Gasch, A.; Eisen, M. *BMC Mol. Biol.* **2006**, *7*, 16.
(15) Yu, X.; Lin, J.; Masuda, T.; Esumi, N.; Zack, D. J.; Qian, J. *Nucleic Acids Res.* **2006**, *34*, 917.
(16) Emami, K. H.; Jain, A.; Smale, S. T. *Genes Dev.* **1997**, *11*, 3007.
(17) Pedersen, A. G.; Baldi, P.; Chauvin, Y.; Brunak, S. *Comp. Biol. Chem.* **1999**, *23*, 191.
(18) Qi, Y.; Bar-Joseph, Z.; Klein-Seetharaman, J. *Proteins: Struct., Funct., Bioinf.* **2006**, *63*, 490.
(19) Kortemme, T.; Baker, D. *Curr. Opin. Chem. Biol.* **2004**, *8*, 91.
(20) Sousa, S. F.; Fernandes, P. A.; Ramos, M. J. *Proteins: Struct., Funct., Bioinf.* **2006**, *65*, 15.
(21) Kitchen, D. B.; Decornez, H.; Furr, J. R.; Bajorath, J. *Nat. Rev. Drug Discovery* **2004**, *3*, 935.
(22) Frederick, K. K.; Marlow, M. S.; Valentine, K. G.; Wand, A. J. *Nature* **2007**, *448*, 325.
(23) Marlow, M. S.; Dogan, J.; Frederick, K. K.; Valentine, K. G.; Wand, A. J. *Nat. Chem. Biol.* **2010**, *6*, 352.
(24) Rinker, S.; Ke, Y.; Liu, Y.; Chhabra, R.; Yan, H. *Nat. Nano.* **2008**, *3*, 418.
(25) Andersen, C. S.; Knudsen, M. M.; Chhabra, R.; Liu, Y.; Yan, H.; Gothelf, K. V. *Bioconjugate Chem.* **2009**, *20*, 1538.
(26) Gauthier, M. A.; Klok, H.-A. *Polym. Chem.* **2010**, *1*, 1352.
(27) Heredia, K. L.; Maynard, H. D. *Org. Biomol. Chem., OBC* **2007**, *5*, 45.
(28) Shakya, A. K.; Sami, H.; Srivastava, A.; Kumar, A. *Prog. Polym. Sci.* **2010**, *35*, 459.
(29) Maheshwari, R.; Levenson, E. A.; Kiick, K. L. *Macromol. Biosci.* **2010**, *10*, 68.
(30) Polizzotti, B. D.; Maheshwari, R.; Vinkenborg, J.; Kiick, K. L. *Macromolecules* **2007**, *40*, 7103.
(31) Hoffman, A. S.; Stayton, P. S.; Bulmus, V.; Chen, G.; Chen, J.; Cheung, C.; Chilkoti, A.; Ding, Z.; Dong, L.; Fong, R.; Lackey, C. A.; Long, C. J.; Miura, M.; Morris, J. E.; Murthy, N.; Nabeshima, Y.; Park, T. G.; Press, O. W.; Shimoboji, T.; Shoemaker, S.; Yang, H. J.; Monji, N.; Nowinski, R. C.; Cole, C. A.; Priest, J. H.; Harris, J. M.; Nakamae, K.; Nishino, T.; Miyata, T. J. *Biomed. Mater. Res.* **2000**, *52*, 577.
(32) Bontempo, D.; Maynard, H. D. *J. Am. Chem. Soc.* **2005**, *127*, 6508.
(33) Alconcel, S. N. S.; Kim, S. H.; Tao, L.; Maynard, H. D. *Macromol. Rapid Commun.* **2013**, *34*, 983.
(34) Platt, V.; Huang, Z.; Cao, L.; Tiffany, M.; Riviere, K.; Szoka, F. C. *Bioconjugate Chem.* **2010**, *21*, 892.
(35) Huang, Z.; Hwang, P.; Watson, D. S.; Cao, L.; Szoka, F. C. *Bioconjugate Chem.* **2009**, *20*, 1667.
(36) Grunwald, C.; Schulze, K.; Reichel, A.; Weiss, V.; Blaas, D.; Piehler, J.; Wiesmüller, K.; Tampé, R. *Proc. Natl. Acad. Sci. U.S.A.* **2010**, *107*, 6146.
(37) Lata, S.; Piehler, J. *Anal. Chem.* **2005**, *77*, 1096.
(38) Tanner, P.; Ezhevskaya, M.; Nehring, R.; Van Doorslaer, S.; Meier, W.; Palivan, C. *J. Phys. Chem. B* **2012**, *116*, 10113.
(39) Rakickas, T.; Gavutis, M.; Reichel, A.; Piehler, J.; Liedberg, B.; Valiokas, R. N. *Nano Lett.* **2008**, *8*, 3369.
(40) Beutel, O.; Nikolaus, J.; Birkholz, O.; You, C.; Schmidt, T.; Herrmann, A.; Piehler, J. *Angew. Chem., Int. Ed.* **2014**, *126*, 1335.
(41) Roullier, V.; Clarke, S.; You, C.; Pinaud, F.; Gouzer, G. r.; Schaible, D.; Marchi-Artzner, V. r.; Piehler, J.; Dahan, M. *Nano Lett.* **2009**, *9*, 1228.
(42) Lata, S.; Gavutis, M.; Tampé, R.; Piehler, J. *J. Am. Chem. Soc.* **2006**, *128*, 2365.
(43) Bhagawati, M.; Lata, S.; Tampé, R.; Piehler, J. *J. Am. Chem. Soc.* **2010**, *132*, 5932.
(44) Grunwald, C.; Schulze, K.; Giannone, G.; Cognet, L.; Lounis, B.; Choquet, D.; Tampé, R. *J. Am. Chem. Soc.* **2011**, *133*, 8090.
(45) Griffith, B. R.; Allen, B. L.; Rapraeger, A. C.; Kiessling, L. L. *J. Am. Chem. Soc.* **2004**, *126*, 1608.
(46) Balland, V.; Hureau, C.; Cusano, A. M.; Liu, Y.; Tron, T.; Limoges, B. *Chem.—Eur. J.* **2008**, *14*, 7186.

(47) Nehring, R.; Palivan, C.; Casse, O.; Tanner, P.; Tu xen, J.; Meier, W. *Langmuir* **2008**, *25*, 1122.
(48) Shepherd, J.; Sarker, P.; Rimmer, S.; Swanson, L.; MacNeil, S.; Douglas, I. *Biomaterials* **2011**, *32*, 258.
(49) Lata, S.; Reichel, A.; Brock, R.; Tampé, R.; Piehler, J. *J. Am. Chem. Soc.* **2005**, *127*, 10205.
(50) Cheng, C.; Schmidt, M.; Zhang, A.; Schlüter, A. D. *Macromolecules* **2006**, *40*, 220.
(51) Singh, G.; Kothari, A. V.; Gupta, V. K. *Polym. Test.* **2009**, *28*, 475.
(52) Yin, X.; Hoffman, A. S.; Stayton, P. S. *Biomacromolecules* **2006**, *7*, 1381.
(53) Mi Kyong, Y.; Yong Kiel, S.; Chong, S. C.; Young, M. L. *Polymer* **1997**, *38*, 2759.
(54) Sellers, R. M.; Williams, W. J. *Farad. Discuss.* **1984**, *77*, 265.
(55) Nishida, Y.; Takahashi, K. *Dalton Trans.* **1988**, 691.
(56) Ellena, J.; Kremer, E.; Facchin, G.; Baran, E. J.; Nascimento, O. R.; Costa-Filho, A. J.; Torre, M. H. *Polyhedron* **2007**, *26*, 3277.
(57) Zhou, S.; Fan, S.; Au-yeung, S. C. F.; Wu, C. *Polymer* **1995**, *36*, 1341.
(58) Wang, Y. M.; Tegenfeldt, J. O.; Reisner, W.; Riehn, R.; Guan, X.-J.; Guo, L.; Golding, I.; Cox, E. C.; Sturm, J.; Austin, R. H. *Proc. Natl. Acad. Sci. U. S. A.* **2005**, *102*, 9796.
(59) Eckhard, U.; Schönauer, E.; Nüss, D.; Brandstetter, H. *Nat. Struct. Mol. Biol.* **2011**, *18*, 1109.
(60) Cairo, C. W.; Gestwicki, J. E.; Kanai, M.; Kiessling, L. L. *J. Am. Chem. Soc.* **2002**, *124*, 1615.
(61) Makeev, V. J.; Lifanov, A. P.; Nazina, A. G.; Papatsenko, D. A. *Nucleic Acids Res.* **2003**, *31*, 6016.
(62) Nehring, R.; Palivan, C.; Moreno-Flores, S.; Mantion, A.; Tanner, P.; Toca-Herrera, J.; Thünemann, A.; Meier, W. *Soft Matter* **2010**, *6*, 2815.
(63) Li, L.; Klim, J. R.; Derda, R.; Courtney, A. H.; Kiessling, L. L. *Proc. Natl. Acad. Sci. U.S.A.* **2011**, *108*, 11745.
(64) De Crescenzo, G.; Pham, P. L.; Durocher, Y.; O'Connor-McCourt, M. D. *J. Mol. Biol.* **2003**, *328*, 1173.
(65) Zaitseva, K. V.; Varfolomeev, M. A.; Novikov, V. B.; Solomonov, B. N. *J. Chem. Thermodyn.* **2011**, *43*, 1083.
(66) Zweep, N.; Hopkinson, A.; Meetsma, A.; Browne, W. R.; Feringa, B. L.; van Esch, J. H. *Langmuir* **2009**, *25*, 8802.
(67) Grünberg, R.; Nilges, M.; Leckner, J. *Structure* **2006**, *14*, 683.
(68) Baldwin, R. L. *J. Biol. Chem.* **2003**, *278*, 17581.
(69) Liao, S.-M.; Du, Q.-S.; Meng, J.-Z.; Pang, Z.-W.; Huang, R.-B. *Chem. Cent. J.* **2013**, *7*, 1.
(70) Cauët, E.; Rooman, M.; Wintjens, R.; Liévin, J.; Biot, C. *J. Chem. Theory Comput.* **2005**, *1*, 472.
(71) Grasberger, B.; Minton, A. P.; DeLisi, C.; Metzger, H. *Proc. Natl. Acad. Sci. U.S.A.* **1986**, *83*, 6258.
(72) Tidor, B.; Karplus, M. *J. Mol. Biol.* **1994**, *238*, 405.
(73) Hsu, S.-T. D.; Blaser, G.; Behrens, C.; Cabrita, L. D.; Dobson, C. M.; Jackson, S. E. *J. Biol. Chem.* **2010**, *285*, 4859.
(74) Anderson, D. E.; Becktel, W. J.; Dahlquist, F. W. *Biochemistry* **1990**, *29*, 2403.